Proceedings of International Structural Engineering and Construction
Holistic Overview of Structural Design and Construction
*Edited by* Vacanas, Y., Danezis, C., Singh, A., and Yazdani, S.

ISSN: 2644-108X

# DESIGN WIND PRESSURE COEFFICIENTS FOR LOW-RISE GABLE-ROOFED STEEL BUILDINGS

SEIYA GUNJI[1], KOSUKE SATO[1], and YASUSHI UEMATSU[2]

[1]*Graduate School of Engineering, Tohoku University, Sendai, Japan*
[2]*National Institute of Technology (KOSEN), Akita College, Akita, Japan*

The present paper discusses the wind pressure coefficients for the main wind force resisting systems of low-rise gable-roofed steel buildings, based on a wind tunnel experiment and a two-dimensional frame analysis. The wind pressure coefficients should be determined so that they reproduce the maximum load effects. Here, focus is on the bending moments involved in the members as the load effects. The Load Response Correlation (LRC) method is employed for evaluating the equivalent static wind pressure coefficients. Using the time history of wind pressure coefficients, the maximum load effects were computed for all combinations of frame location and wind direction. The results indicate that the most critical condition occurs on the windward frame in a diagonal wind. The largest bending moment was compared with that predicted from the wind pressure coefficients specified in the Japanese building standards, which are based on the area-averaged mean wind pressure coefficients. Finally, more reasonable wind pressure coefficients for designing the main wind force resisting systems are proposed.

*Keywords*: Low-rise steel structure, Wind tunnel experiment, Main wind force resisting system, Load effect.

## 1 GENERAL APPEARANCE

The external pressure coefficients for designing the structural frames of low-rise buildings with gable roofs are provided in the Recommendations for Loads on Buildings (2015) published by the Architectural Institute of Japan (AIJ 2015). The wind pressure coefficients are specified only for two wind directions normal to the walls. However, the effects of wind direction within a range of the designated direction ± 45° is considered in the specifications. Indeed, the mean values of the area-averaged wind pressure coefficients over the load bearing area of column or beam for various frame locations and wind directions within the above-mentioned range are plotted against roof pitch, and the specified values are determined so as to envelope the plotted data. Therefore, the specified values for the walls and roofs are not necessarily obtained from the results for the same wind direction. Furthermore, they are not based on the load effects on the structure.

In the present study, the external pressure coefficients for the main wind force resisting systems are investigated based on a wind tunnel experiment and a two-dimensional frame analysis, focusing on the load effects. The validity of the provisions in the AIJ Recommendations are also examined. Finally, more reasonable wind pressure coefficients are proposed based on the present results.

## 2 WIND TUNNEL EXPERIMENT

### 2.1 Target Building

The target building is a one-story gable-roofed steel structure. The structure consists of a series of planar moment frames arranged in parallel and connected by horizontal beams. The dimension is as follow; span $B$ = 12 m, length $W$ = 24 m, spacing of frames $d$ = 6 m, mean roof height $H$ = 4.5 m – 9.0 m (4 types), and roof pitch $\beta$ = 0° – 30° (4 types).

### 2.2 Experimental Apparatus and Procedure

The experiment was carried out in an Eiffel-type boundary layer wind tunnel at the Department of Architecture and Building Science, Tohoku University, which has a working section of 1.4 m width, 1.0 m height and 6.5 m length. The wind tunnel models were made with a geometric scale of $\lambda_L$ = 1/100. Figure 1 shows a development view of the wind tunnel model and the location of pressure taps, which are arranged along Lines 1 – 3. The mean roof height $H$ was varied from 4.5 to 9.0 cm by sinking the model under the wind tunnel floor. Therefore, the total number of pressure taps along a line ranges from 12 to 20 depending on $H$.

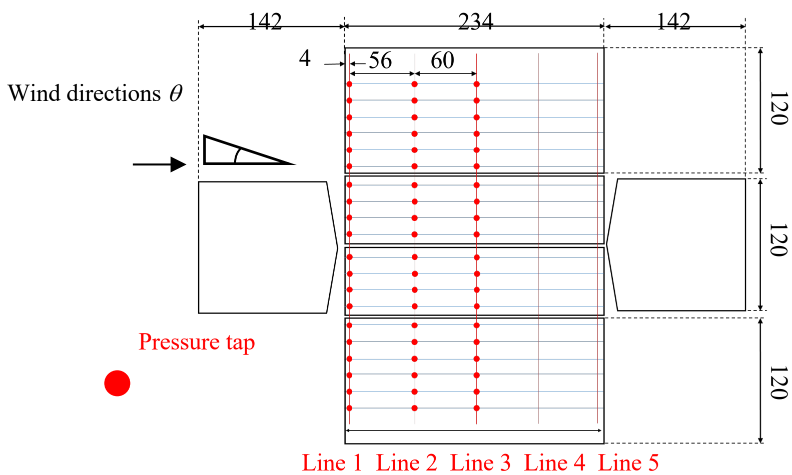


Figure 1. Experimental model and pressure tap location (unit: mm).

The wind tunnel flow is a turbulent boundary layer with a power law exponent of $\alpha$ = 0.27. The turbulence intensity $I_{uH}$ at the mean roof height $H$ is in a range from 0.19 to 0.22. Assuming that the 'basic wind speed' $U_0$, specified in the AIJ Recommendations, is 35 m/s, which covers almost the whole area of Japan, and the terrain category is III (open-country exposure), the design wind speed $U_H$ at the mean roof height $H$ is calculated as $U_H$ = 24.3 m/s because $H < Z_b$ (= 10 m, with $Z_b$ being a height specified for each terrain category in the AIJ Recommendations). In the wind tunnel experiment, the mean wind speed $U_H$ at the mean roof height $H$ was changed with $H$ so that the wind speed scale $\lambda_V$ became 1/4. Thus, the time scale is calculated as $\lambda_T$ = 1/25. The sampling frequency for pressure measurements was 500 Hz. The time duration for evaluating the statistics of pressure coefficients and load effects is 10 minutes in full scale. Note that the statistics are evaluated by applying ensemble average to the results of the 6 runs. The wind direction $\theta$, defined as shown in Figure 1, was changed from 0° to 180° at a step of 15°. The wind pressure $p$ is reduced to the external pressure coefficient $C_p$ defined as follows in Eq. (1):

$$C_p = \frac{p - p_s}{q_H} \tag{1}$$

where $p_s$ represents the static pressure, and $q_H$ the velocity pressure at the mean roof height $H$. The $C_p$ distributions along Lines 4 and 5 are obtained from the results for Lines 2 and 1 respectively, considering the symmetry of the building.

### 2.3 Results for the Mean Wind Pressure Coefficients

In order to understand the basic characteristics of external pressures acting on the building, the distributions of mean wind pressure coefficients $\bar{C}_p$ were obtained. Figure 2 shows the results for typical wind directions when $\beta$ = 20° and $H$ = 7.5 m. Note that each figure shows the development view of the $\bar{C}_p$ distribution on the roof and side walls.

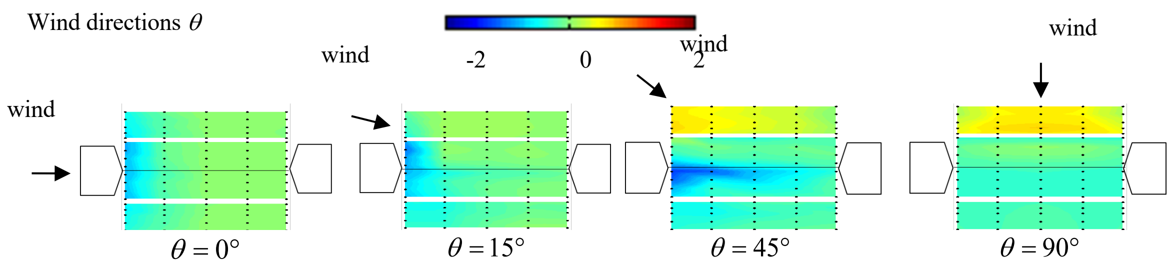


Figure 2. Distributions of the mean wind pressure coefficients for typical wind directions.

When $\theta$ = 0° – 45°, large negative pressures are induced in a wide area near the windward gable wall. In particular, when $\theta$ = 30° – 45°, an area of the leeward roof near the ridge is subjected to very large suctions. This is due to the generation of conical vortices. These results are consistent with those of previous researches.

## 3 VERIFICATION OF THE SPECIFIED VLUES IN THE AIJ RECOMMENDATIONS

### 3.1 Model of Analysis

The frames are assumed to be constructed of H-section steel members of SN400B, specified in the Japanese Industrial Standards (JIS), with a yield stress of $\sigma_y$ = 235 N/mm$^2$. Two types of column bases, i.e., 'pinned' and 'clumped', are assumed. The cross section of the members is determined based on the short-term allowable stress design, in which the loads are provided by the AIJ Recommendations. Table 1 shows the size and sectional properties of the members in the case where the column base is clumped to the foundation. It is assumed that the cross section of members does not depend on the roof pitch.

Table 1. Size and sectional properties of the members (clamped column base).

| Height $H$ (m) | Member size (mm) | Cross section (mm$^2$) | Mass per unit length (kg/m) | Moment of inertia (mm$^4$) | Section modulus (mm$^3$) |
|---|---|---|---|---|---|
| 4.5 – 7.5 | 300×175×7×11 | $6.29\times10^3$ | 49.4 | $1.35\times10^8$ | $7.71\times10^5$ |
| 9.0 | 300×200×8×12 | $7.11\times10^3$ | 55.8 | $1.11\times10^8$ | $7.56\times10^5$ |

### 3.2 Load Effects Under Consideration for Estimating Design Wind Loads

In the case of relatively rigid low-rise steel structures, where the resonance effect of fluctuating wind pressures is neglected, the load effect to be considered in the wind load estimation can be obtained from the stress analysis of the structure under static wind loading (Yasushi 2004). That is, the most critical stress involved in the members under static wind loading can be used as the load effect under consideration for estimating the design wind loads. Such an analysis indicated that the critical load effect was the bending moment at the base for the clumped-base structure, while it is the bending moment at the knee for the pinned-base structure. The bending moment $M(t)$ of concern is given by Eq. (2) as follows:

$$M(t) = q_H \sum_{j=1}^{n} \alpha_j C_{p,j} A_j \tag{2}$$

where $n$ is the total number of pressure taps; $j$ is the tap index; $A_j$ is the load bearing area of Tap $j$; $C_{p,j}$ represents the wind pressure coefficient at Tap $j$; and $\alpha_j$ is the influence coefficient, or the bending moment of concern when unit load is applied to the frame at the location of Tap $j$. Note that the internal pressure coefficient is assumed 0. For given $\beta$, $H$ and column-base condition, the maximum peak value of $M(t)$ during a time duration of 10 min in full scale was obtained by using Eq. (2). Table 2 summarizes the frame number (the frame number is represented by the line number) and the wind direction $\theta_{cr}$ that provide the most critical value of the bending moment together with the corresponding gust effect factor $G_f$ in the case of $\beta = 10°$. In general, the largest bending moment was induced in the frame along Line 2 (see Figure 1) in an oblique wind. This is because the oblique wind generates such a wind pressure distribution on Frame 2, which is asymmetric with respect to the ridge. Accordingly, in the following sections, focus is on the bending moment induced in Frame 2 in oblique winds for discussing the design wind loads.

Table 2. The condition providing the most critical value of the bending moment ($\beta = 10°$).

| ***H*** **(m)** | **Pinned column-base** | | | **Clamped column-base** | | |
|---|---|---|---|---|---|---|
| | **Frame** | $\boldsymbol{\theta_{cr}}$ **(°)** | $\boldsymbol{G_f}$ | **Frame** | $\boldsymbol{\theta_{cr}}$ **(°)** | $\boldsymbol{G_f}$ |
| 4.5 | 2 | 60 | 2.44 | 2 | 60 | 2.86 |
| 6.0 | 2 | 60 | 2.41 | 2 | 75 | 3.04 |
| 7.5 | 2 | 60 | 2.22 | 2 | 60 | 2.68 |
| 9.0 | 2 | 60 | 2.04 | 2 | 75 | 2.71 |

### 3.3 Validation of the Specifications in the AIJ Recommendations for Loads on Buildings

In the AIJ Recommendations, the external pressure coefficients are specified for two wind directions, labelled as 'W1' and 'W2', parallel and normal to the ridge. Regarding the bending moment, the wind direction 'W2' provides more critical value. Hence, focus is on this wind direction in the present paper. The maximum bending moment, $M^*_{cr}$, involved in the frame calculated from the specified values of the AIJ Recommendations is compared with that obtained from the time history of wind pressure coefficients. The results for $\beta = 10°$ and 30° are shown in Figure 3. In the figure 'Experiment' indicates the experimental value of $M^*_{cr}$ divided by $G_f$, while 'Recommendations' indicates the value calculated from the specified external pressure coefficients without considering $G_f$.

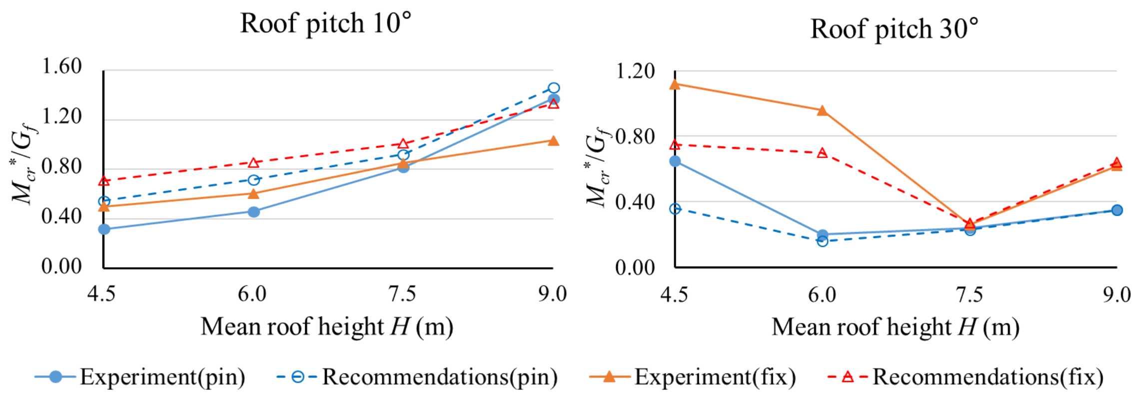


Figure 3. Maximum load effects obtained from the experimental data and the AIJ Recommendations of $C_p$ plotted as a function of $H$ (Frame 2).

When $\beta \leq 20°$, the 'Recommendations' values are approximately 2.5 times larger than those of 'Experiment', indicating that the AIJ Recommendations overestimate the design wind loads significantly. By comparison, the 'Recommendations' values are smaller than those of 'Experiment' when $\beta = 30°$. These results imply that the actual wind pressure distribution producing the maximum load effect is different from that assumed in the AIJ Recommendations.

## 4 PROPOSAL OF EXTERNAL PRESSURE COEFFICIENTS BASED ON THE MAXIMUM LOAD EFFECTS

### 4.1 Distributions of Equivalent Static Wind Pressure Coefficients Based on LRC Method

In order to obtain the distribution of equivalent static pressure coefficients, $C_{p\_\mathrm{LRC}}$, providing the maximum load effect, the LRC (Load Response Correlation) method is employed (Kasperski 1992). This method considers the correlation between the load effect and the wind pressures acting on the frame. $C_{p\_\mathrm{LRC}}$ is provided by Eq. (3) as follows:

$$C_{p\_\mathrm{LRC}} = \bar{C}_p + g_r C'_p \rho_{rp} \tag{3}$$

where $\bar{C}_p$ = mean external pressure coefficient; $g_r$ = peak factor of the load effects; $\rho_{rp}$ = correlation coefficients between the external pressure and the load; and $C'_p$ = RMS value of fluctuating wind pressure coefficient.

Next, the $C_{p\_\mathrm{LRC}}$ distributions obtained for the two column-base conditions were applied to the frames with these column-base conditions and the maximum bending moment was computed. Comparing the results with each other, it was found that the $C_{p\_\mathrm{LRC}}$ distribution for the pinned column-base provided larger bending moment than that for the clumped column-base. Therefore, the $C_{p\_\mathrm{LRC}}$ distribution for the pinned column-base is used for proposing the design wind pressure coefficients.

The process for proposing the design wind pressure coefficients is as follow. First, the $C_{p\_\mathrm{LRC}}$ distribution is averaged over the windward wall, windward roof, leeward roof and leeward wall. Then, considering that the practical $C_{p\_\mathrm{LRC}}$ distribution on each area is not uniform, the effect of such a difference in the pressure coefficient on the maximum bending moment is taken into account by introducing a correction factor $\gamma$, which is defined by the ratio of the bending moment obtained from the practical $C_{p\_\mathrm{LRC}}$ distribution and that obtained from the area-averaged values.

In the framework of the gust effect factor approach, which is generally used in the current building codes and standards of many countries, the design wind pressure coefficient is provided by the product of the area-averaged $C_{p\_\mathrm{LRC}}$ value and the correction factor $\gamma$, divided by the gust effect factor. Table 3 shows the wind pressure coefficients obtained by the above-mentioned procedure, in which $C_{p\_WU}$, $C_{p\_RU}$, $C_{p\_RL}$ and $C_{p\_WL}$ represent the proposed wind pressure coefficients for the windward wall, windward roof, leeward roof and leeward wall, respectively.

Table 3. Proposed wind pressure coefficients for the main wind force resisting system.

| $\beta$(°) | $H$ (m) | $C_{p\_WU}$ | $C_{p\_RU}$ | $C_{p\_RL}$ | $C_{p\_WL}$ | $\beta$(°) | $H$ (m) | $C_{p\_WU}$ | $C_{p\_RU}$ | $C_{p\_RL}$ | $C_{p\_WL}$ |
|---|---|---|---|---|---|---|---|---|---|---|---|
| 0 | 4.5 | 0.43 | –0.31 | –0.31 | –0.24 | 20 | 4.5 | 0.44 | –0.08 | –0.70 | –0.22 |
| | 6.0 | 0.51 | –0.37 | –0.37 | –0.28 | | 6.0 | 0.51 | –0.09 | –0.66 | –0.25 |
| | 7.5 | 0.61 | –0.42 | –0.42 | –0.34 | | 7.5 | 0.55 | –0.15 | –0.63 | –0.28 |
| | 9.0 | 0.64 | –0.46 | –0.46 | –0.33 | | 9.0 | 0.57 | –0.18 | –0.61 | –0.31 |
| 10 | 4.5 | 0.52 | –0.38 | –0.29 | –0.17 | 30 | 4.5 | 0.35 | 0.08 | –1.15 | –0.25 |
| | 6.0 | 0.55 | –0.40 | –0.26 | –0.19 | | 6.0 | 0.37 | 0.13 | –0.83 | –0.27 |
| | 7.5 | 0.60 | –0.63 | –0.42 | –0.35 | | 7.5 | 0.22 | 0.01 | –0.76 | –0.30 |
| | 9.0 | 0.62 | –0.68 | –0.44 | –0.36 | | 9.0 | 0.24 | 0.00 | –0.77 | –0.34 |

The value of $C_{p\_WU}$ is generally positive. The sign of $C_{p\_RU}$ changes from negative to positive as the roof pitch $\beta$ increases. This is due to the change in flow separation point from the windward eaves to the ridge. When $\beta$ = 30°, the flow separates at the ridge, generating large suctions on the leeward roof. These features correspond well to the tendency of the mean wind pressure coefficient distribution, as shown in Figure 2.

## 5 CONCLUDING REMARKS

The wind pressure coefficients for the main wind force resisting systems of low-rise gable-flamed steel structures have been discussed based on a wind tunnel experiment and a 2D frame analysis, assuming that the structure consists of a series of moment frames arranged in parallel. The effects of roof pitch, frame position, column base conditions, and wind direction on the maximum bending moment (load effect under consideration) were made clear. It was found that the most critical value was induced on the windward frame in an oblique wind. The distribution of equivalent static wind pressure coefficients providing the maximum load effect under such a condition was calculated by using the LRC method. Finally, more reasonable specification of the wind pressure coefficients has been proposed based on the results.

## References

*AIJ, Recommendations for Loads on Buildings (2015)*, Architectural Institute of Japan, Tokyo, 2015.

Kasperski, M., *Extreme Wind Load Distributions for Linear and Non-Linear Design*, Engineering Structures, 14(1), 27-34, 1992.

Yasushi, U., Toshiyasu, O., Shunichiro, W., Shuji, K. and Masaru, I., *Wind Loads on a Steel Greenhouse with a Wing-Like Cross Section*, Proceedings of the 18th National Symposium on Wind Engineering, 347-352, 2004.